Climatological Relationship between Warm Season Atmospheric Rivers and Heavy Rainfall over East Asia

著者別名	釜江 陽一
journal or publication title	Journal of the Meteorological Society of Japan
volume	95
number	6
page range	411-431
year	2017-11
権利	(C)2017, Meteorological Society of Japan
URL	http://hdl.handle.net/2241/00149341

doi: 10.2151/jmsj.2017-027

Supplement for "Climatological relationship between warm season atmospheric rivers and heavy rainfall over East Asia"

by Youichi Kamae, Wei Mei, and Shang-Ping Xie

Supplement 1

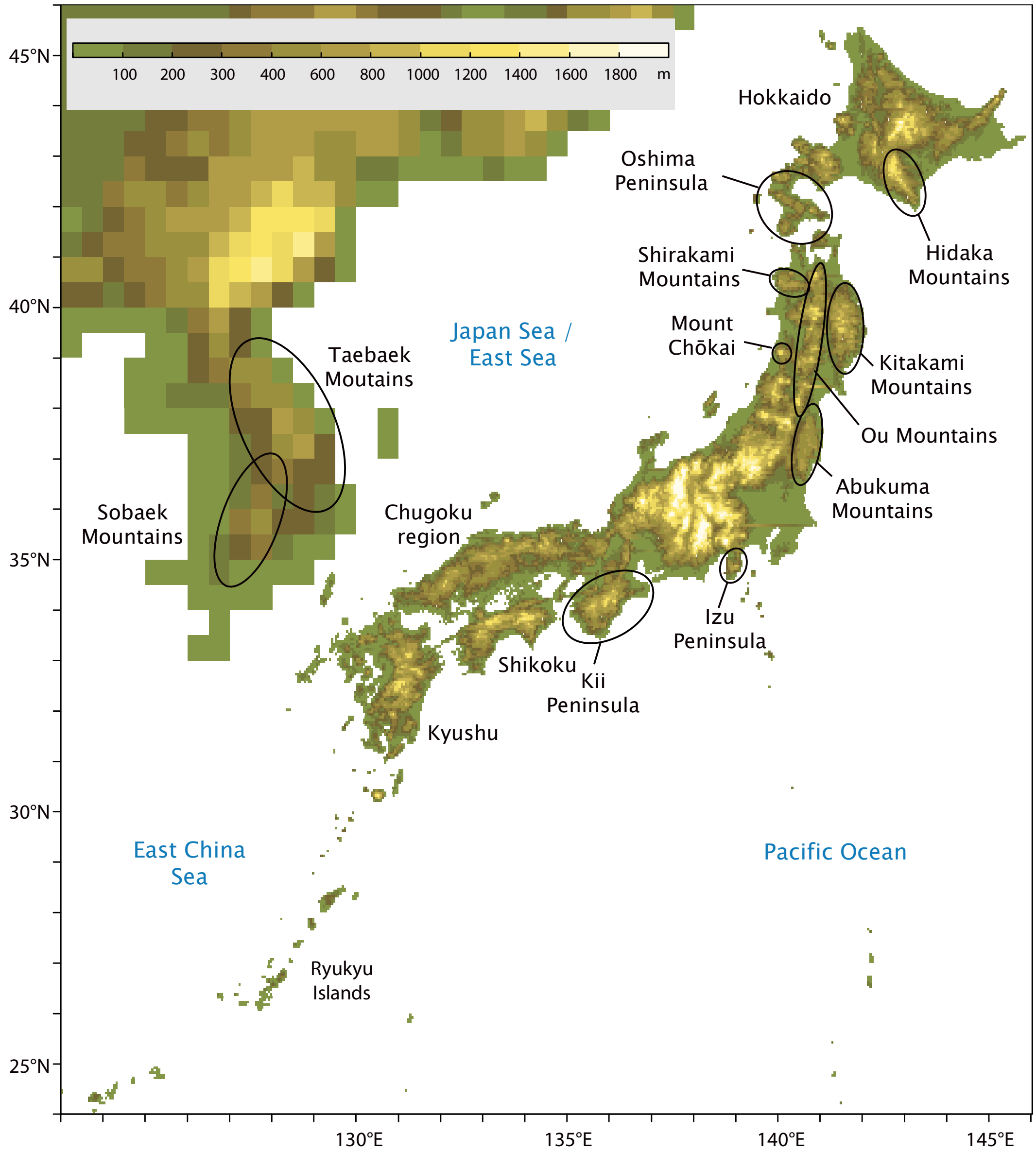

Fig. S1 Geographical names over the Korean Peninsula and Japan used in this study. Resolutions of topography over the Eurasian Continent and Japan are 0.5° × 0.5° and 0.05° × 0.05°, respectively (identical to Fig. 1).

Supplement 2

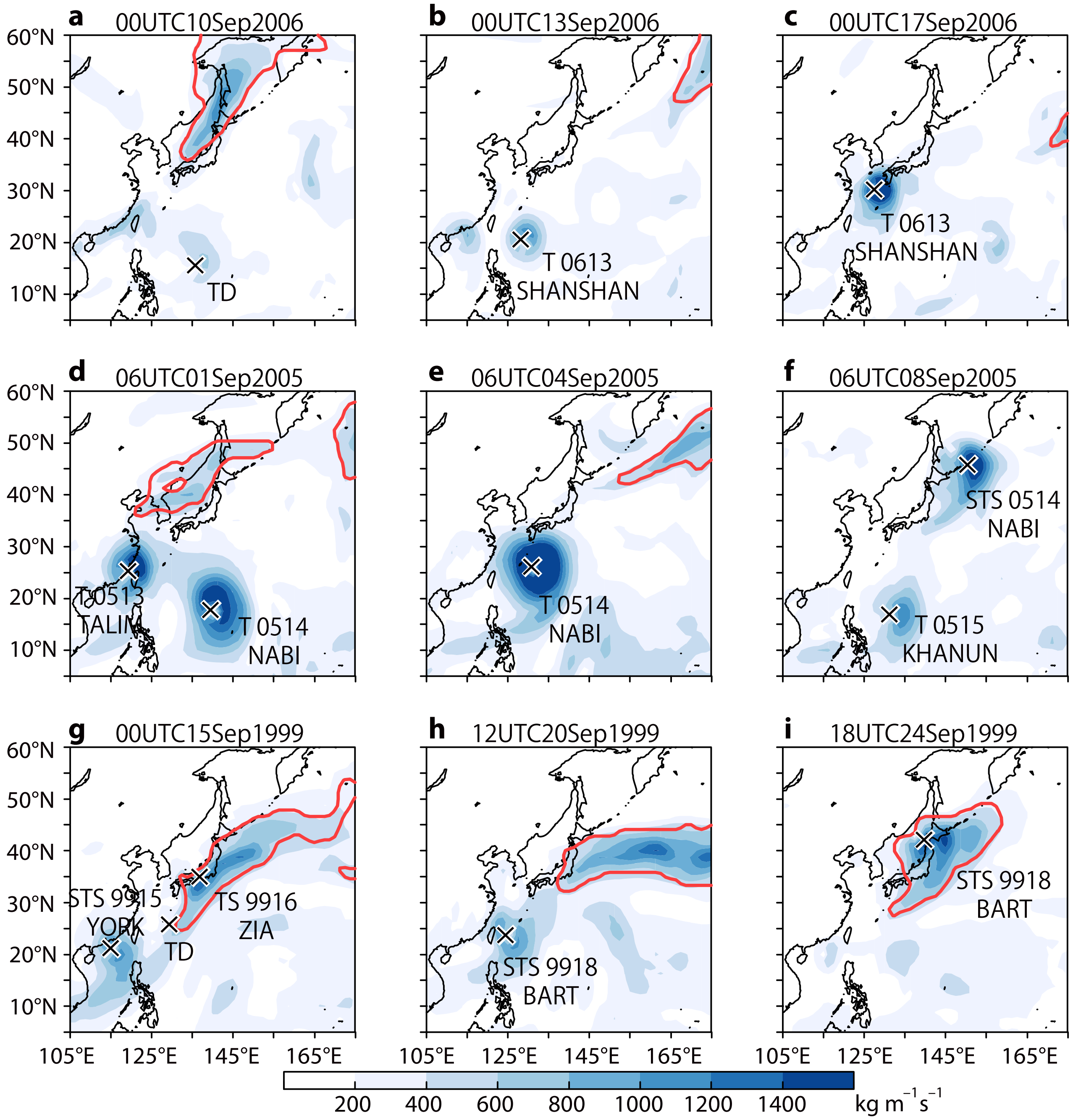

Fig. S2 Examples of East Asian tropical cyclones with or without ARs. IVT (shading; kg m^{-1} s^{-1}) and detected ARs (red outlines) at (a) 00UTC 10 Sep 2006, (b) 00UTC 13 Sep 2006, (c) 00UTC 17 Sep 2006, (d) 06UTC 01 Sep 2005, (e) 06UTC 04 Sep 2005, (f) 06UTC 08 Sep 2005, (g) 00UTC 15 Sep 1999, (h) 12UTC 20 Sep 1999, and (i) 18UTC 24 Sep 1999. Cross marks represent centers of tropical cyclones. TD, TS, STS, and T indicate tropical depression, tropical storm, severe tropical storm, and typhoon.

Tropical cyclones over the Northwestern Pacific often bring intense water vapor flow and associated heavy rainfall over East Asia via its local or remote (e.g. predecessor rain events; Galarneau et al. 2010) effects. In some cases, it is difficult to separate such moisture transport bands from East Asian ARs. The AR detection method employed in this study simply excludes local effects of tropical cyclones by applying several IVT-band criteria (area, length, and length/width ratio; see section 2.2). Figure S2 shows some examples of IVT fields associated with tropical cyclones and their relationships with ARs. In the first two cases (Figs. S2a–f), ARs occurred over mid-latitude East Asia and then moved eastward, with tropical cyclones developing to their south/southwest. These AR events can be considered independent of tropical cyclones. In contrast, during September 1999, IVT bands extending from tropical cyclones over the Northwestern Pacific merged with mid-latitude moisture bands, resulting in an elongated AR over East Asia (Fig. S2g). On September 24, the IVT associated with tropical storm BART was counted as an AR event. This suggests that the IVT-band criteria (area, length, and length/width ratio; see section 2.2) employed in this study *sometimes* are not effective in distinguishing IVT associated with (the local effects of) *weak* tropical cyclones from the conventional mid-latitude ARs, although this takes place rarely. Including other criteria (e.g. temperature anomalies in the upper troposphere) in the detection algorithm might be helpful. Further efforts to distinguish IVT associated with (the local effects of) *weak* tropical cyclone from conventional ARs are important for better evaluation of AR effects on regional climate system and natural hazards over the Northwestern Pacific, North Atlantic, and other regions with frequent tropical cyclones.

Supplement 3

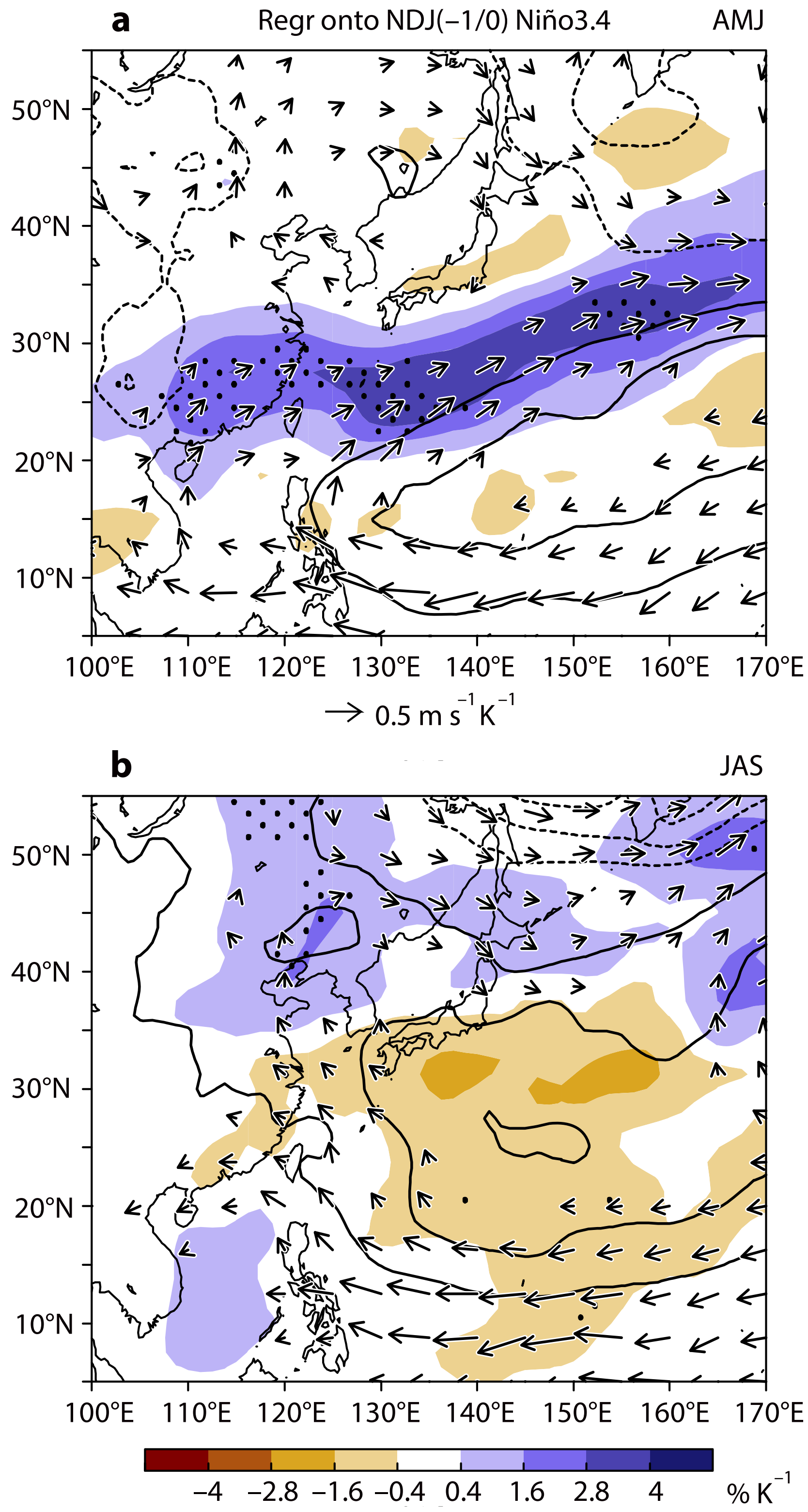

Fig. S3 Similar to Fig. 12, but for 1958–1978.

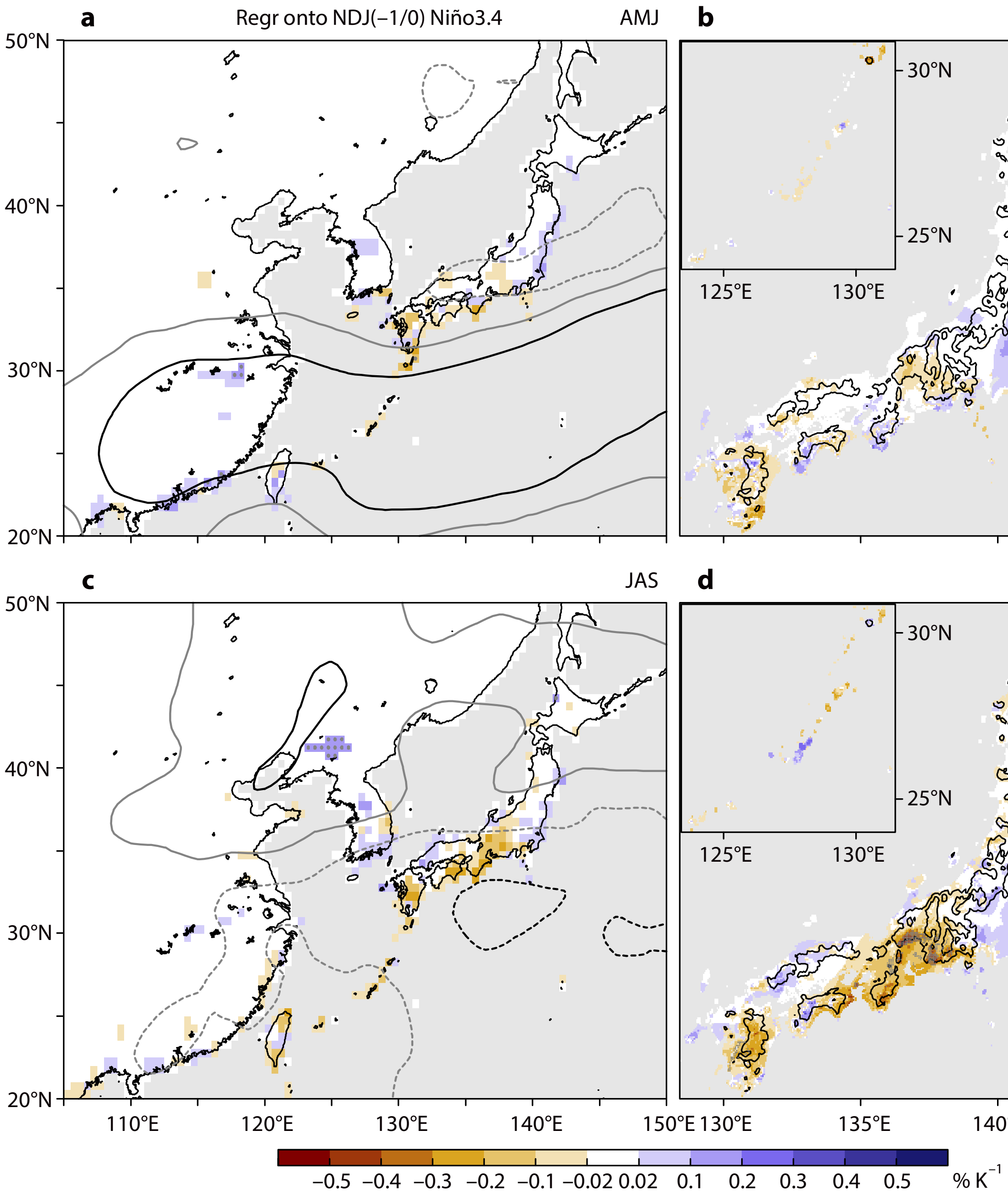

Fig. S4 Similar to Fig. 13, but for 1958–1978.

The coupling of summertime East Asian atmospheric circulation and the preceding-winter ENSO shows a substantial interdecadal variation across the 1970s. Figures S3 and S4 show lagged relationship of spring-to-summer East Asian atmospheric circulation, AR frequency, and frequency of AR-related heavy rainfall with preceding-winter

ENSO for 1958–1978. During this period, the TWNP anticyclone in post-El Niño spring (Fig. S4a) contributed by local air-sea interactions (Wang et al. 2000) is found, consistent with the period after the 1970s (Fig. 12a). In contrast, the anomalous TWNP anticyclone (Fig. 12b) is not found around the Philippines in JAS (Fig. S3c), resulting in a distinct pattern of anomalous AR frequency and frequency of heavy rainfall (Fig. S4) to the post 1970s.

Xie et al. (2010) explained that the different atmospheric responses in the post-El Niño seasons before and after the 1970s are consistent with difference in background thermocline depth in the tropical Southwest Indian Ocean. Kubota et al. (2016) found similar interdecadal modulations (the 1910s, 1930s, and 1970s) of relationship between ENSO and the PJ pattern based on long-term station and ship-based observation data. Xie et al. (2016) provided a review on the interdecadal modulations of ENSO-Asian climate coupling. The interdecadal modulations indicate that the lagged effect of ENSO on East Asian AR occurrence (and AR-related heavy rainfall) found during the period since the 1970s possibly vary in the future. These results highlight the importance of continuous monitoring of global climate variability and regional climate extremes to more reliable decadal and interdecadal climate predictions.

References

Galarneau, T. J. Jr., L. F. Bosart, and R. S. Schumacher, 2010: Predecessor rain events ahead of tropical cyclones. *Mon. Wea. Rev.*, **138**, 3272–3297.

Kamae, Y., W. Mei, S.-P. Xie, M. Naoi, and H. Ueda, 2017: Atmospheric rivers over the Northwestern Pacific: Climatology and interannual variability. *J. Climate*, **30**, 5605–5619.

Kubota, H., Y. Kosaka, and S.-P. Xie, 2016: A 117-year long index of the Pacific-Japan pattern with application to interdecadal variability. *Int. J. Climatol.*, **36**, 1575–1589.

Wang, B., R. Wu, and X. Fu, 2000: Pacific–East Asia teleconnection: How does ENSO affect East Asian climate? *J. Climate*, **13**, 1517–1536.

Xie, S.-P., Hu, K., J. Hafner, H. Tokinaga, Y. Du, G. Huang, and T. Sampe, 2009: Indian Ocean capacitor effect on Indo-western Pacific climate during the summer following El Niño. *J. Climate*, **22**, 730–747.

Xie, S.-P., Y. Du, G. Huang, X.-T. Zheng, H. Tokinaga, K. M. Hu, and Q. Y. Liu, 2010: Decadal shift in El Niño influences on Indo–Western Pacific and East Asian climate in the 1970s. *J. Climate*, **23**, 3352–3368.